

Preparation of WO₃ Nano-material Negative Electrode for Asymmetric Supercapacitor

Wei XU¹, Gui XU², Deng-Liang WANG¹, Jin-Tian LIN¹, Yu BAI¹, Li-Te ZHAO, Jing-Quan MO and Dong-Hua FAN^{1*}

¹School of Applied Physics & Materials, Wuyi University, Jiangmen 529020, China

²Baotou Power Supply Bureau, Jianshe Road, Baotou, Inner Mongolia 014030, China⁴

* Corresponding author's e-mail: donghua_fan@126.com

Keywords: Nanomaterial WO₃; Thermal evaporation method; Asymmetric supercapacitors; Negative electrode materials;

Abstract. Tungsten oxide nanomaterials were deposited on flexible conductive carbon fiber sheets by a simple thermal evaporation method and compared with conventional hydrothermal tungsten oxide nanomaterials. The morphology and composition of the product were characterized by X-ray diffraction and scanning electron microscope. The electrochemical properties of WO₃ nano-electrode materials were tested by three-electrode system. The results showed that the area capacitance of WO₃ nanoelectrode was 0.24F/cm² at a current density 10mA/cm², which was similar to that of tungsten oxide composite electrode prepared by complex evaporation plating process. After charging and discharging, the capacitance retention rate can be maintained about 80%, proving that WO₃ nanocrystalline has large capacitance, good redox reversibility and electrochemical stability, and can be used as negative electrode material for asymmetric supercapacitors.

Introduction

Energy storage devices with high efficiency have given rise to lots of attention because of more and more urgent demand for environmental conservation and coping with the increasingly serious depletion of fossil fuels [1]. The rapid development in high-power electronic devices, emergency power supplies and hybrid electric vehicles provide the potential application for these energy storage devices [2, 3]. Among them, the advent of supercapacitors (SCs) as a new class of energy storage appeal for a large amount of scientists due to their advantages of high-power density, excellent reversibility, fast recharge ability, and long cycle life[4,5]. However, encountered with the problem of low energy density, the further application of supercapacitors is under restrictions. On account of the equation of energy density, $E = 0.5 CV^2$, to increase the energy density of SCs, it is essential to augment the output voltage and/or the capacitance [6]. It is effective to increase the voltage up to 3V using organic and ionic liquid electrolytes, such as lithium perchlorate in propylene carbonate or tetraethyl ammonium tetrafluoroborate in acetonitrile, but the enhancement of voltage is at the high cost, poor ionic conductivity, and high toxicity [7].

An alternative to increasing voltages is developing asymmetric supercapacitors (ASCs) with a battery type Faradaic positive electrode as energy source and a capacitive negative electrode as a power source, together with environmentally friendly aqueous electrolytes which have higher ionic conductivities. Different from symmetric supercapacitors (SSCs), by combining the voltage windows of two different electrodes, ASCs are able to increase the maximum operation voltage up to 2V in aqueous electrolyte, and thus power and energy density of the device.

For all great progress made in improving the capacitance of positive electrode materials, the research on negative electrode materials is seldom carried out [8, 9]. Even of Carbon-based nanomaterials are commonly used as negative electrode in virtue of their high surface area, excellent electrical conductivity, and large power density [7], their low specific capacitance weakens the further enhancement of the energy density for ASCs. Therefore, it is desired to search novel negative electrode materials for ASCs.

Some negative electrodes based on metal oxide such as Co₃O₄/RuO₂, [10,11] MoO_{3-x}, [12], V₆O₁₃ [13] and iron oxide [14] have shown much higher energy density than carbon-based

materials; However, they suffered from the low electronic conductivity, which has a negative impact on their electrochemical performance. In order to address this problem, the selection of high-specific surface area and high-conductivity nanomaterials, such as tungsten oxide (WO_{3-x}) nanowires, [15, 16] to load electrochemically active materials is worth considering. However, the research on using tungsten oxide for supercapacitors is relatively few because it is hard to grow this kind of nanomaterials by conventional hydrothermal method due to its high melting points.

In this communication, we reported a different method from hydrothermal synthesis, which is depositing tungsten oxide (WO_3) by evaporation. In addition, the performance of the negative electrode materials using the two methods will be compared. The capacitance performance of WO_3 nanomaterial as negative electrode is improved markedly when deposited, achieving areal capacitance of 0.24 F/cm^2 at current density of 10 mA/cm^2 and capacitance retention of 80% after 10000 cycles at a scan rate of 200 mV/s .

Experimental

All reagents used in the experiment are up to the standard of analytical grade that were used without any further purification. The WO_3 samples were fabricated on a carbon cloth substrate by using hydrothermal method and evaporation method separately. First group, 10 mmol of $\text{Na}_2\text{WO}_4 \cdot 2\text{H}_2\text{O}$, 30 mmol of NH_4F , and 25 mmol of $\text{CO}(\text{NH}_2)_2$ were dissolved in 60 mL of DI water under stirring, respectively. After 10 minutes of slight stirring, two Teflon-lined stainless-steel autoclaves of 25 mL capacity were filled with 20 mL of homogeneous solution prepared above respectively. Then, carbon clothes ($2 \text{ cm} \times 3 \text{ cm}$) were cleaned by ethanol, deionized water, and using ultrasonic treatment in turn and then immersed into the reaction solution. Subsequently, the two autoclaves were sealed and heated at 120°C for 12 hs (Sample 1) and 150°C for 12hs (Sample 2) and then allowed to cool down to room temperature. Second group, 20 mmol of $\text{Na}_2\text{WO}_4 \cdot 2\text{H}_2\text{O}$, 20 mmol of Na_2SO_4 , and were dissolved in 40 mL of DI water under stirring, respectively. The autoclave was sealed and heated at 160°C for 24 hs (Sample 3). Third group, 20 mmol of $\text{Na}_2\text{WO}_4 \cdot 2\text{H}_2\text{O}$ and 20 mmol of NaCl were dissolved in 40 mL of DI water under stirring, respectively adjusting the solution to $\text{PH}=2$ with HCL solution. The autoclave was sealed and heated at 160°C for 24 hs (Sample 4). The other process of Sample 3 and 4 are the same as Sample 1 and 2.

Two cleaned carbon clothes used as substrate were cleaned by ethanol, deionized water, the 0.65g of ultrafine tungsten powder was placed onto the bottom of tungsten boat evenly and then ethanol was dripped into the powder to avoid the powder dropping out when the boat is upside down. Put the boat and the carbon clothes to their corresponding position in evaporation coating machine. The flow rate is that Argon flow 60sccm and Oxygen flow 0.5SCCM. After 20 minutes of venting, Evaporation power starts to heat the boat with the rate of 1A/s . The temperature rose to 1120°C , remaining for 15 minutes and then stop heating. The sample E was taken out after the 15 minutes of cooling.

Material Characterization and Electrochemical Measurement

The composition morphology and structure of the electrode materials were characterized by X-ray diffraction patterns, and Field emission SEM (FE-SEM, JSM-6330F). CV and galvanostatic charge/discharge measurements were conducted using an electrochemical workstation (CHI 660D). The electrochemical measurements were performed in a three-electrode cell, with the individual sample used as the working electrode, a Carbon rod as the counter electrode and a SCE as the reference electrode.

Results and Discussion

Figure 1 shows the X-ray diffraction (XRD) patterns of the sample 1 and sample5, indicating that the peaks of both samples. Can be indexed to the standard card (JCPDS Card No. 05-0388), which are in accordance with Tungsten Oxide (WO_3).

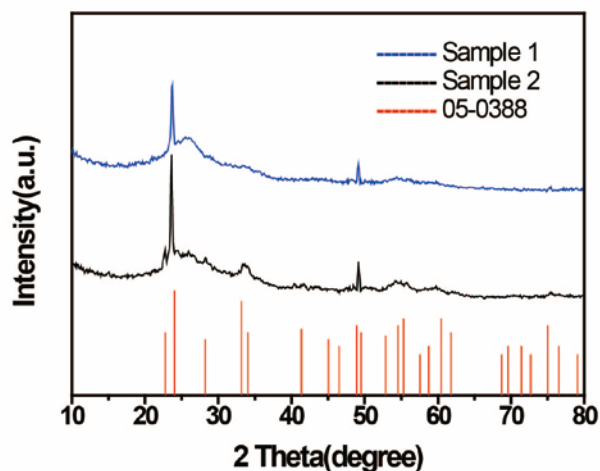


Fig. 1 XRD spectra collected for WO_3 electrodes.

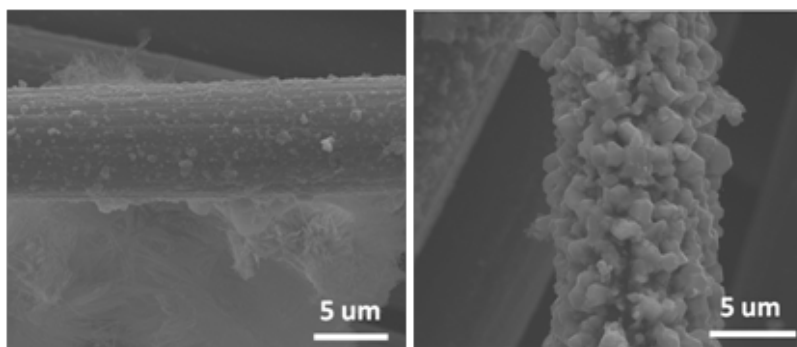


Fig. 2 SEM images of (a) WO_3 nanomaterials by hydrothermal, (b) WO_3 nanomaterials by evaporation on a carbon cloth

The SEM images of WO_3 on the carbon clothes of Sample1 and Sample2 are shown in Figures 2(a), (b) respectively. It can be observed from Figure 1a that the carbon fibers were dotted with not a few WO_3 nano-particles on Sample 1 by hydrothermal method, with a diameter about 1nm. In contrast, it can be seen in Figure 2(b) that the distribution of WO_3 nano-particles in Sample5 are more uniform than that in Sample1, with a diameter about 2nm and the number much more than that of WO_3 nano-particles in Sample1, indicating that evaporation deposition is more beneficial to the growth of WO_3 nano-particles than hydrothermal method. As a result, the specific surface area got increased on electrode materials, combined with the high conductivity of carbon fiber, and the capacitance of the negative electrode is, therefore, augmented.

The electrochemical properties of the WO_3 electrodes were investigated in a three-electrode cell in 5 M LiCl aqueous electrolyte, with a Carbon rod counter-electrode and a SCE reference electrode. Cyclic voltammogram (CV) curves of WO_3 electrodes for Sample 1, 2, 3 and 4 at a scan rate of 100 mV/s were compared in Figure 3(a). It is clear that the area of the CV curve for Sample 1 is larger than that for other three samples, and furthermore, the CV profiles of the Sample 1 at various scan rates remain similar as the scan rate increases from 10 to 200 mV/s (Figure 3(b)), indicating that hydrothermal process used for Sample1 is more suitable than that for other samples.

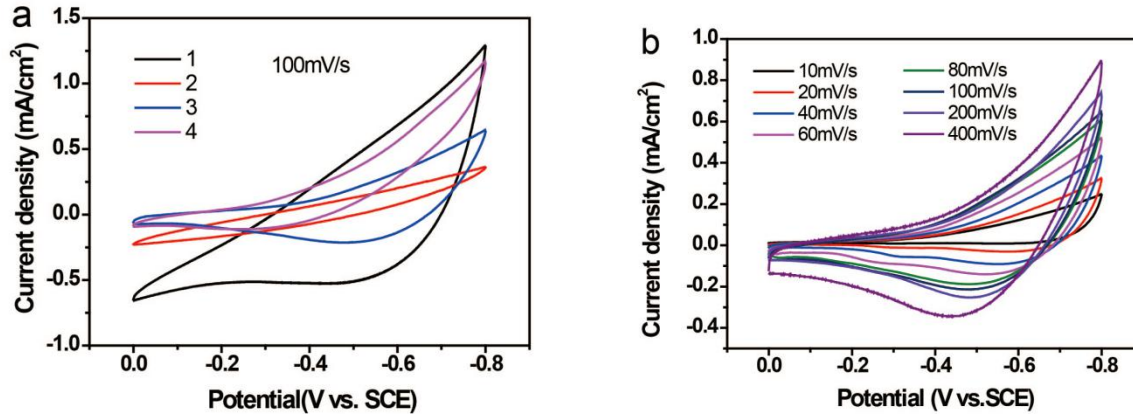


Fig. 3 (a) CV curves collected for Sample 1, 2, 3 and 4 negative electrodes at a scan rate of 100 mV/s. (b) CV curves collected for Sample 1 negative electrode at various scan rates.

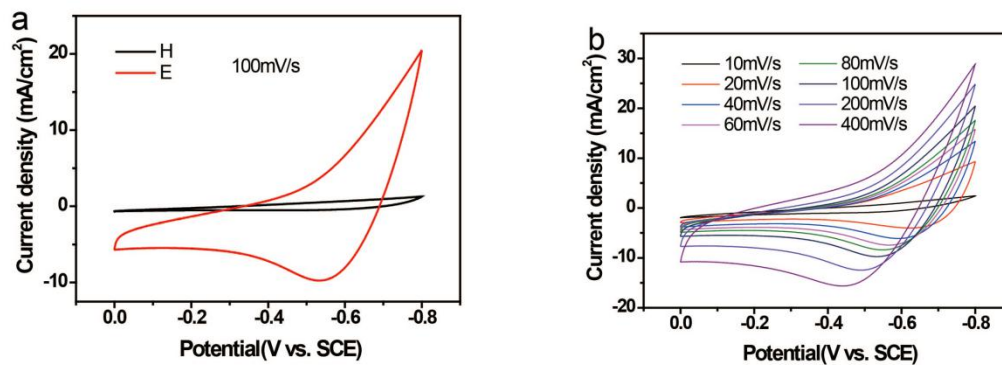


Fig. 4 (a) CV curves collected for WO₃ negative electrodes by both hydrothermal(H) and evaporation(E) method at a scan rate of 100 mV/s. (b) CV curves collected for WO₃ negative electrodes by evaporation(E) method at various scan rates.

Cyclic voltammetry (CV) curves of Sample1 (noted as H) and Sample5 (noted as E) electrodes at a scan rate of 100 mV/s are compared in Fig. 4a. As is shown, the current density of the evaporation Sample5 electrode is substantially higher than that of the Hydrothermal Sample1 electrode, indicating that the substantial enhancement of electrochemical capacitance originated from the a mass of growth of WO₃ nano-particles by evaporation process. Moreover, it can be observed in Fig.4b that the CV curves of the Sample5 at various scan rates remain similar as the scan rate increases from 10 to 400 mV/s, making it clear the significantly enhanced capacitive properties and high-rate capability of the WO₃ electrode by evaporation process.

Figure 5 illustrates the areal capacitances of the Sample5 at the scan rates from 10 mV/s to 400 mV/s calculated on the basis of its CV curves, which is the same order of magnitudes as what was reported about negative electrode for ASCs in Advanced Energy Materials. The fabrication of WO₃ electrode is much simpler than that of WO_{3-x}/MoO_{3-x} electrode.

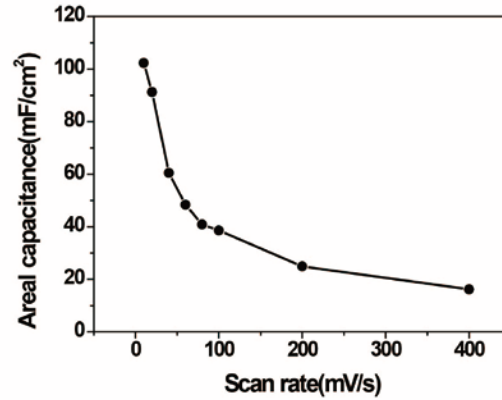


Fig. 5 Areal capacitance of the WO_3 negative electrode as a function of the scan rate.

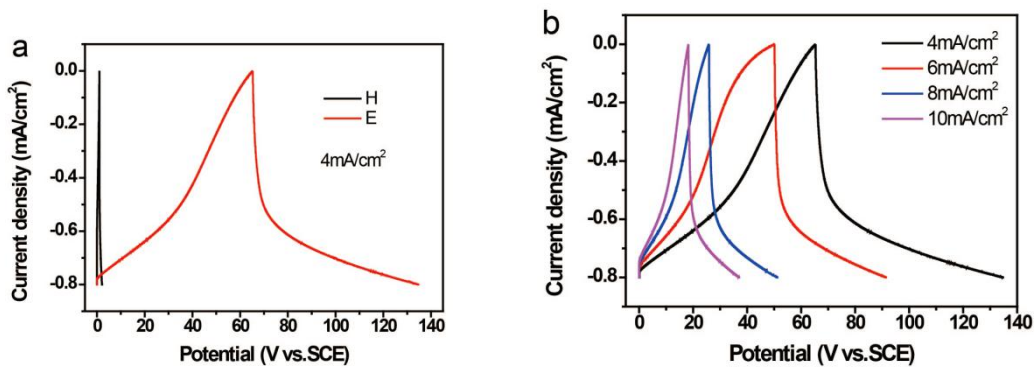


Fig. 6 (a) Galvanostatic charge-discharge curves of the WO_3 negative electrodes by both hydrothermal (H) and evaporation (E) method at 4 mA/cm^2 . (b) Galvanostatic charge-discharge curves of the WO_3 negative electrodes by evaporation collected at different current densities.

The galvanostatic charge-discharge curves of the Sample1 and Sample5 electrodes at a current density of 4 mA/cm^2 are shown in Figure 6(a). Compared with Sample1, Sample 5 exhibits slower and more symmetrical charge and discharge curves and a more linear variation of potential vs. time, which is also supported by the galvanostatic charge-discharge curves collected for Sample5 electrode at different current densities from 2 to 3, 4, 5, 6, 8, and 10 mA/cm^2 (Figure 6(b)), proving the greatly improved capacitance, Columbic efficiency, and reversibility of the WO_3 electrode at a high current density by evaporation process.

The areal capacitance of 0.24 F/cm^2 at current density of 10 mA/cm^2 (shown in Figure 7(a)) can be up to $\text{WO}_{3-x}/\text{MoO}_{3-x}$ electrode (about 0.24 F/cm^2), the best value for WO_3 . Figure 7(b) shows the capacitance retention of Sample5 as a function of cycle number. The capacitance retention of WO_3 is still about 80% of the original capacitance after 10000 cycles at a scan rate of 200 mV/s , indicating that WO_3 by evaporation is of excellent long cycle life, demonstrating that WO_3 by the evaporation process in this paper is a suitable candidate for negative electrode.

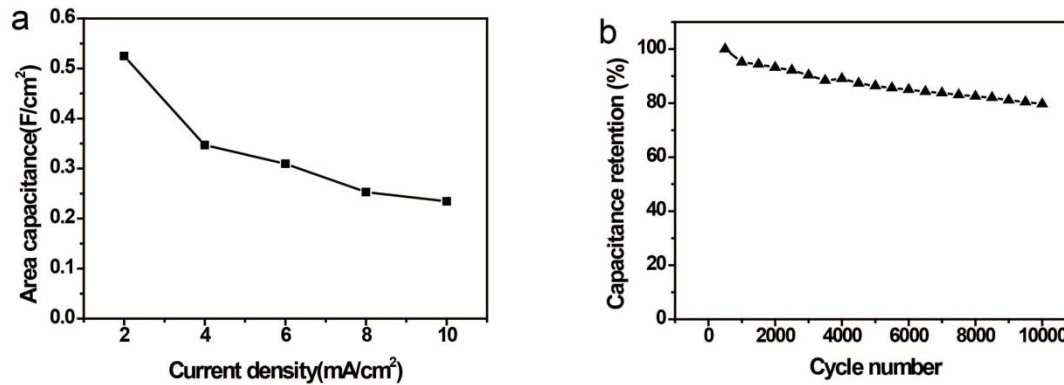


Fig. 7 (a) Areal capacitance of the WO_3 negative electrodes by evaporation collected from galvanostatic charge-discharge curves as a function of current density. (b) Cycling performance of the WO_3 negative electrodes by evaporation at 200 mV/s for 10000 cycles

Conclusion

In conclusion, a feasible method has been explored to grow WO_3 nanomaterials on carbon clothes by evaporation. The electrochemical performances of WO_3 negative electrode have been significantly improved by changing the fabrication process from conventional hydrothermal method to evaporation method. Moreover, stable rate capability and cycle capability were also achieved. These encouraging performances have access to its applications in high-performance asymmetric super-capacitors, opening up a novel approach to advancing the performance of energy storage devices. Moreover, stable rate capability and cycle capability were also achieved. These encouraging performances have access to its applications in high-performance asymmetric super-capacitors, opening up a novel approach to advancing the performance of energy storage devices.

Acknowledgments

The authors acknowledge the financial support from Guangdong province innovation and strong school project (2016KTSCX142), Guangdong University Innovation Team Project (2015KCXTD027), Special Funds for the Cultivation of Guangdong College Students' Scientific and Technological Innovation ("Climbing Program" Special Funds.) (pdjh2017b0519), China's Postdoctoral Science Foundation (no. 2013M540744), Natural Science Foundation of Shanxi Province, China (2014JM7265), Degree and Postgraduate Education Reform Project of Wuyi University (no.30641015). This work was supported by Science Foundation for Young Teachers of Wuyi University (2015zk13), The Mobilization Project of Scientific and Technological Equipment (Yue Cai-Jiao [2015] 356), Guangdong Self Financing Science and Technology Project (Yue Ke-Cai [2015] 110: Research and development of high strength environmentally-friendly halogen-free flame retardant PBT composites).

References

- [1] MAHLIA T, SAKTISAHDAN T, JANNIFAR A, et al. A review of available methods and development on energy storage; technology update [J]. *Renewable and Sustainable Energy Reviews*, 2014, 33:532-45.
- [2] a, SIMON P, GOGOTSI Y. Materials for electrochemical capacitors [J]. *Nat Mater*, 2008, 7(11): 845-54;
- [3], Naoi K, Simon P. New Materials and New Configurations for Advanced Electrochemical Capacitors. *J. Electrochem. Soc.*, 2008, 17: 34-37.

- [4] P.Simon, Y. Gogotsi, B. Dunn. Where do batteries end and supercapacitors begin? *Science*. 2014, 343(6150), 1210-1211.
- [5] PECH D, BRUNET M, DUROU H, et al. Ultrahigh-power micrometre-sized supercapacitors based on onion-like carbon [J]. *Nature nanotechnology*, 2010, 5(9): 651-4.
- [6] FANG B, WEI Y, MARUYAMA K, et al. High capacity supercapacitors based on modified Activated carbon aerogel [J]. *J Appl Electrochem*, 2005, 35(3): 229-33.
- [7] A. Lewandowski, A. Olejniczak, M. Galinski, and I. Step-niak, "Performance of carbon-carbon supercapacitors based on organic, aqueous and ionic liquid electrolytes," *Journal of Power Sources*, vol. 195, no. 17, pp. 5814–5819, 2010.
- [8] Z. Fan, J. Yan, T. Wei et al., "Asymmetric supercapacitors based on graphene/MnO₂ and activated carbon nanofiber electrodes with high power and energy density," *Advanced Functional Materials*, vol. 21, no. 12, pp. 2366–2375, 2011.
- [9] W.-H. Jin, G.-T. Cao, and J.-Y. Sun, "Hybrid supercapacitor based on MnO₂ and columned FeOOH using Li₂SO₄ electrolyte solution," *Journal of Power Sources*, vol. 175, no. 1, pp. 686–691, 2008.
- [10] J. Xu, Q. Wang, X. Wang, Q. Xiang, B. Hang, D. Chen and G. Shen, *ACS Nano*, 2013, 7, 5453-5452.
- [11] Wei Xu, Jiahui Chen, Minghao Yu, Yinxiang Zeng, Yongbing Long, Xihong Lu, and Yexiang Tong, "Sulphur-doped Co₃O₄ Nanowires as Advanced Negative Electrode for High-energy Asymmetric Supercapacitors", *Journal of Materials Chemistry A*, 2016, 4, 10779-10785.
- [12] J. Chang, M. Jin, F. Yao, T. Kim, V. Le, H. Yue, F. Gunes, B. Li, A. Ghosh, S. Xie and Y. H. Lee, *Adv. Funct. Mater.* 2013, 23, 5074-5082.
- [13] T. Zhai, X. Lu, Y. Ling et al., "A new benchmark capacitance for supercapacitor anodes by mixed-valence sulfur-doped V₆O₁₃," *Advanced Materials*, vol. 26, no. 33, pp. 5869–5875, 2014.
- [14] X. Lu, Y. Zeng, M. Yu, T. Zhai, C. Liang, S. Xie, M. Balogun, and Y. Tong, *Adv. Mater.*, 2014, 26, 3148–3155.
- [15] X. H. Lu, T. Zhai, X. H. Zhang, Y. Q. Shen, L. Y. Yuan, B. Hu, L. Gong, J. Chen, Y. H. Gao, J. Zhou, Y. X. Tong, Z. L. Wang, *Adv. Mater.* 2012, 24, 938.
- [16] Xu Xiao, Tianpeng Ding, Jun Zhou, etc, "WO_{3-x}/MoO_{3-x} Core/Shell Nanowires on Carbon Fabric as an Anode for All-Solid-State Asymmetric Supercapacitors" *Advanced Energy Materials*, vol. no. pp. 5869–5875, 2012.